SLAC-PUB-7169
May 1996

Effects of Multiple Scattering and Target Structure on Photon Emission *

Richard Blankenbecler

Stanford Linear Accelerator Center
Stanford University, Stanford, California 94309
e-mail: rzbth@slac.stanford.edu

Abstract

The Landau-Pomeranchuk-Migdal effect is the suppression of Bethe-Heitler radiation caused by multiple scattering in the target medium. The quantum treatment given by S. D. Drell and the author for homogeneous targets of finite thickness will be reviewed. It will then be extended to structured targets. In brief, it is shown that radiators composed of separated plates or of a medium with a spatially varying radiation length can exhibit unexpected structure, even coherence maxima and minima, in their photon spectra. Finally, a functional integral method for performing the averaging implicit in multiple scattering will be briefly discussed and the leading corrections to previous results evaluated.

Presented at the 3rd AUP Workshop on
Quantum Chromodynamics: Collisions, Confinement, and Chaos
American University of Paris, Paris, France, June 3-8 1996.

*Work supported by the Department of Energy, contract DE-AC03-76SF00515.

1 Introduction and Motivation

In a paper[1] by S. D. Drell and the author, a quantum treatment of multiple scattering and of the bremsstrahlung of photons by a charged particle undergoing random multiple scattering was given. This treatment included as limiting cases the familiar Bethe-Heitler (BH) radiation[2] from a charged particle scattering from an isolated atom relevant for a thin target, and in the opposite limit the Landau-Pomeranchuk[3]-Migdal[4] (LPM) effect which has been experimentally verified[5] to suppress the radiation for a thick target. This formulation included the effects of a finite target thickness in such a way as to smoothly connect these two limits. An eikonal approach was used and lead to a physical but quantum mechanical treatment of multiple scattering and then to a derivation of the LPM suppression of soft photon radiation from high energy electrons in matter.

The physics of the LPM effect is that of the formation length of the photon; this is, the longitudinal path length required via the uncertainty relation for a high energy electron of initial momentum p, final momentum p', and mass m, to radiate a photon of momentum k near the forward direction. The formation length is given by $l_f = 2pp'/(m^2k)$. At high energies ($p,\ p' >> m$) and for soft photon emission $k << p$, the formation length l_f can grow quite large relative to the scattering mean free path of the electron, eventually becoming macroscopic. When this occurs, there is a loss of coherence that leads to suppression in spite of the net increase in the amount of acceleration of the charge.

A general and clear treatment of semiclassical photon radiation can be found in the review paper by A.I. Akhiezer and N. F. Shul'ga[9] where earlier references can be found. A more accurate treatment of the coulomb nature of the basic scattering process has recently been given[10] for an infinite target.

2 Eikonal Results and Statistics of the Medium

We need not review in detail the eikonal formulation for high energy scattering by extended targets[1]. Suffice it to say that since we are interested in the effects of multiple scattering in the medium, the eikonal expansion must be carried out to order $(1/p$ in order to include the effects of 'bending' of the particle paths. The phase functions will involve longitudinal integrals through the scattering fields of the target. The main perturbation on the trajectory arises from the transverse electric fields of the atoms in the medium. For simplicity we model the non-crystalline medium in the following way. Consider an electron entering the medium. As it wanders through the medium, it will experience transverse forces due to atoms randomly above or below its path and at varying distances or strengths. The next electron incident upon the target will enter at a different point and see a completely different set of varying fields. While each electron sees a fixed set of fields, the ensemble of incident particles will see an almost random set. Clearly, the probability of the particular process under study must be computed for fixed fields, and then these fields must be statistically averaged. The eikonal approach is convenient, because one can write down the transition probabilities in closed form, and then perform the averaging explicitly.

The matrix element for single photon emission using the above approximations and the probability for emission were fully discussed[1]. The result for a given field distribution in the target was given in the form, $p_f = x\,p_i$ and $k = (1-x)\,p_i$,

$$\frac{\pi(1-x)}{\alpha x}\,\frac{dP(x)}{dx} \;=\; I \;=\; \int_{-\infty}^{\infty} db_2 \int_{-\infty}^{b_2} db_1\, I(b_2, b_1, b_l)\ , \tag{1}$$

where

$$I(b_2, b_1, b_l) \;=\; 2\,\frac{C(b_2)C(b_1)}{b}\left\{\left[1 + \frac{1}{2}r(x)\lambda(b_2, b_1, b_l)\right]\sin(c) - \sin(b)\right\}\ ,$$

$$c = b[1+\eta(b_2,b_1,b_l)]\,, \tag{2}$$

and the dimensionless variables are defined by $b_i = z_i/l_f$ and $b = b_2 - b_1$.

The field dependent quantities $\lambda(z_2,z_1,l)$ and $\eta(z_2,z_1,l)$ are given by

$$z^2 m^2 \eta(z_2,z_1,l) = z\int_{z_1}^{z_2} dz[\vec{A}_\perp(z,z_1)]^2 - [\int_{z_1}^{z_2} dz\,\vec{A}_\perp(z,z_1)]^2\,, \tag{3}$$

$$m^2\lambda(z_2,z_1,l) = [\vec{A}_\perp(z_2,z_1)]^2 \tag{4}$$

$$\text{with} \qquad \vec{A}_\perp(z_2,z_1) = \int_{z_1}^{z_2} dz'\,\vec{E}_\perp(z')\,, \tag{5}$$

and where $z = z_2 - z_1$.

The model introduced in Ref. [1] reflects the fact that each incident electron experiences a very different arrangement of the atomic electric fields. The statistical average involved is therefore the average over the wave packets of the individual electrons. The transverse field varies with depth z from atomic layer to atomic layer. The quantity $\vec{E}_\perp(z)dz$ is simply the differential transverse momentum acquired in traversing the medium from z to $z + dz$. Its statistical average in this non-crystalline medium is given by

$$\left\langle \vec{E}_\perp(z_2)\cdot\vec{E}_\perp(z_1)\right\rangle = \frac{<\vec{p}_\perp^{\,2}>}{L(z_2)}\,\delta(z_2-z_1)\,. \tag{6}$$

where explicit note has been taken that the medium may vary from layer to layer so that the radiation length may depend upon position. This relation allows one to compute all statistical averages that will be needed. The average transverse momentum accumulated in one radiation length of target is $<\vec{p}_\perp^{\,2}> = 2\pi m^2/\alpha$.

The transverse electric field is zero outside the region $0 < z < l$ where l is the total thickness of the target. To lowest order, used by LPM for example, the statistical averages for the needed quantities can be computed directly from the above:

$$\langle\lambda(b_2,b_1,b_l)\rangle = l_f\frac{2\pi}{\alpha}\int_{b_1}^{b_2}\frac{db'}{L(b')} \tag{7}$$

$$\langle\eta(b_2,b_1,b_l)\rangle = l_f\frac{2\pi}{\alpha}\int_{b_1}^{b_2}\frac{db'}{L(b')}\frac{(b_2-b')(b'-b_1)}{b^2}\,, \tag{8}$$

where $b = b_2 - b_1$. $L(z)$ is the radiation length that is taken to be infinite outside the target, i.e., for $z < 0$ and for $z > l$. Recognizing αL as the mean free path, it is convenient to introduce the thickness of the target in units of the average inverse mean free path as

$$T = l_f \frac{\pi}{3\alpha} \int_0^{b_l} \frac{db'}{L(b')} = \frac{\pi}{3\alpha} \int_0^{l} \frac{dz'}{L(z')} . \tag{9}$$

This allows the overall scales to be extracted from λ and η. To this end define

$$\langle \lambda(b_2, b_1, b_l) \rangle = 6\, T\, \bar{\lambda}(b_2, b_1, b_l) \tag{10}$$

$$\langle \eta(b_2, b_1, b_l) \rangle = 6\, T\, \bar{\eta}(b_2, b_1, b_l) , \tag{11}$$

where

$$\bar{\lambda}(b_2, b_1, b_l) = \frac{1}{J} \int_{b_1}^{b_2} \frac{db'}{L(b')} \qquad J = \int_0^{b_l} \frac{db'}{L(b')} \tag{12}$$

$$\bar{\eta}(b_2, b_1, b_l) = \frac{1}{J} \int_{b_1}^{b_2} \frac{db'}{L(b')} \frac{(b_2 - b')(b' - b_1)}{b^2} . \tag{13}$$

The explicit statistical averages for a homogeneous target plate of thickness l are readily evaluated. The results for b_2 and b_1 in the regions before, inside, and after the target, denoted by (– , 0 , +) respectively, are

Region $(b_2\, b_1)$	$\lambda(b_2, b_1, b_l)$	$6\, b^2\, \bar{\eta}(b_2, b_1, b_l)$	$12\, b^2\, \bar{\delta}(b_2, b_1, b_l)$
$(- -)$	0	0	0
$(+ +)$	0	0	0
$(0\ -)$	b_2/b_l	$b_2^2\,[3b - 2b_2]/b_l$	$b_2^3\,[4b - 3b_2]/b_l^2$
$(+\ 0)$	$(b_l - b_1)/b_l$	$(b_l - b_1)^2\,[3b - 2(b_l - b_1)]/b_l$	$(b_l - b_1)^3\,[4b - 3(b_l - b_1)]/b_l^2$
$(0\ \ 0)$	b/b_l	b^3/b_l	b^4/b_l^2
$(+ -)$	1	$[3(b_2 + b_1)b_l - 2b_l^2 - 6b_2 b_1]$	$[4b_2 b_l + 2b_1 b_l - 3b_l^2 - 12 b_2 b_1]$

These formulas join smoothly at all common boundaries of the regions. In addition, the symmetry between (+) and (–) , that is $(b_2 \leftrightarrow b_l - b_1)$, is also evident.

3 Functional Integrals

In order to evaluate the statistical average of the probability of emission to all orders, in is convenient to introduce a standard functional averaging procedure used in the

treatment of gaussian random variables. The probability of emission, or rather the integrand $I(b_2, b_1, b_l)$, is averaged over the distribution

$$< I(b_2, b_1, b_l) > = \frac{1}{Z} \int [dE_\perp]\, I(b_2, b_1, b_l) \ , \tag{14}$$

where

$$[dE_\perp] = [d^2 E_\perp] \exp[- \int dz_1 dz_2 E_\perp(z_2) W(z_2, z_1) E_\perp(z_1)] \ . \tag{15}$$

The unit matrix weight W reflects that there is zero correlation length in z, or more precisely that it is small compared to the mean free path and the formation length. The inverse of W measures the size of the electric field fluctuations,

$$W(z_2, z_1) = \frac{\alpha}{2\pi m^2} L(z_2)\, \delta(z_2 - z_1) \ . \tag{16}$$

Since the function $I(b_2, b_1, b_l)$ involves the electric field in a quadratic functional inside a trigometric function, the statistical average is easily performed. The leading correction to the LPM approximation involves a cross correlation between the amplitude term $\bar{\lambda}$ and the phase term $\bar{\eta}$. This new term, denoted by $\bar{\delta}$, is given in the previous table. Explicitly it is

$$\bar{\delta}(b_2, b_1, b_l) = \frac{1}{J^2 b^2} \int_{b_1}^{b_2} \frac{db'}{L(b')} \frac{db''}{L(b'')} [b(b_2 - b_>) - (b_2 - b')(b_2 - b'')] \ , \tag{17}$$

where $b_>$ is the greater of b' or b'' and J is the normalization integral used in Eq. (13).

4 Emission Probability

In Ref.[1], the statistical average of the probability of emission was evaluated in the LPM approximation, which simply replaces the field quantities $\lambda(b_2, b_1, b_l)$ and $\eta(b_2, b_1, b_l)$ by their averages. This approximation is not necessary[12] as seen in the previous section, and the lowest order cross correlation between the amplitude and

phase can be easily evaluated. Eliminating the integration variable b_1 in favor of b yields

$$< I(b_2, b_1, b_l) > \;=\; 2\frac{C(b_2)C(b_1)}{b}\Big\{[1 + 3\,r(x)\,T\,\bar{\lambda}(b_2, b_1, b_l)]\,\sin(c) - \sin(b) + 9\,r(x)\,T^2\,\bar{\delta}(b_2, b_1, b_l)\,b\,\cos(c)\Big\}\,, \qquad (18)$$

$$\text{where} \qquad c \;=\; b\,[\,1 + 6\,T\,\bar{\eta}(b_2, b_1, b_l)\,]\,. \qquad (19)$$

To this order, the only difference from the result of Ref. [1] is the $\cos(c)$ term that arose from the cross correlation. Now the numerical effect of this term will be discussed.

5 Bethe-Heitler Limit and LPM Form Factor

To first order in $\bar{\lambda}$ and $\bar{\eta}$, each of which is proportional to the square of the net impulse given to the radiating particle, the integrand is

$$I_{\rm BH}(b_2, b_1, b_l)_1 \;=\; 6\,T\,\frac{C(b_2)C(b_1)}{b}\,\Big\{r(x)\bar{\lambda}(b_2, b_1, b_l)\,\sin(b) + 2\,\bar{\eta}(b_2, b_1, b_l)b\,\cos(b)\Big\}\,. \qquad (20)$$

Using the above values for $\bar{\lambda}$ and $\bar{\eta}$ and interchanging the integration order yields

$$I(\mathrm{BH}) \;=\; 2\,\mathrm{T}\int_{-\infty}^{\infty}\mathrm{dbC(b)}\,\{3\,\mathrm{r(x)}\,\sin(\mathrm{b}) + \mathrm{b}\,\cos(\mathrm{b})\} \;=\; 2\,\mathrm{T}\,[3\,\mathrm{r(x)} - 1] \to 4\,\mathrm{T}\,. \qquad (21)$$

This is the familiar BH formula in the soft photon limit. This result, as expected, does not depend upon the detailed structure or geometric arrangement of the target, only the total number of radiation lengths through the target as expressed by the integral T. In Ref. [1] a form factor *F*, which is unity when BH is valid, was introduced to track the LPM suppression. Here it is convenient to define

$$< I > \;=\; I(\mathrm{BH})\;\mathrm{F(k, T, x)}\,, \qquad (22)$$

where the x dependence arises only from the spin factor $r(x)$ and *T* is essentially the number of mean free paths through the target. The photon momentum k together

with the particle energy determine the formation length l_f . The form factor is given by

$$F(k,T,x) \;=\; \int_{-\infty}^{\infty} db \int_{-\infty}^{\infty} db_2\, F(b_2,b,b_l)\ , \tag{23}$$

$$\text{where}\quad F(b_2,b,b_l) \;=\; \frac{C(b)}{2\,T\,b}\Big\{[1+3\,r(x)\,T\,\bar{\lambda}(b_2,b_2-b,b_l)]\,\sin(c)-\sin(b) \\ +9\,r(x)\,T^2\,\bar{\delta}(b_2,b_2-b,b_l)\,b\,\cos(c)\Big\}\ . \tag{24}$$

6 Small k Limit

The BH limit is valid for small *T* and small formation lengths (or large k); the macroscopic internal structure of the target plays no role here. In the small *k* limit, in which the formation length becomes larger than the target thickness, the internal structure of the target again plays no role. However the suppression due to multiple scattering is still manifest. Also, in the limit of extremely small *k,* the effects of the index of refraction of the target medium become important; these effects are not treated here. Our problem becomes one of radiation from a effectively thin target. In this limit one finds

$$\begin{aligned}
\bar{\lambda}(b_2,b_1,b_l) &\sim \theta(b_2-B)\theta(B+b-b_2) \\
\bar{\eta}(b_2,b_1,b_l) &\sim \bar{\lambda}(b_2,b_1,b_l)\,(b_2-B)(B+b-b_2)/b^2 \\
\bar{\delta}(b_2,b_1,b_l) &\sim \bar{\lambda}(b_2,b_1,b_l)\,[b(b_2-B)-(b_2-B)^2]/b^2\ ,
\end{aligned} \tag{25}$$

where *B* is the position of the center of the target. Writing $b_2 = B + bw$ with $db_2 = b\,dw$, allows the *b* integral to be performed and the form factor becomes

$$F(l_f >> l,T,r) \;\sim\; \frac{1}{2T}\int_0^1 dw\,\left\{(1+\frac{3}{2}rT)/D(w)+\frac{3}{2}rT/D^2(w)-1\right\}\ , \tag{26}$$

where *D(w)* = 1 + $6Tw(1-w)$. For $T \to 0$, the form factor approaches one, the BH result. For finite *T,* the form factor is below the BH value. Again, this result does

not depend upon the detailed structure or geometric arrangement of the target, only on the integral variable T.

7 Structured Target

The cases of a thin, finite and thick homogeneous targets were discussed in Ref.[1]. It is straightforward to numerically integrate the explicit formula for the form factor F for any target configuration. Here we will discuss the radiation from segmented or laminated targets that are composed of identical plates separated by a vacuum gap of constant width. The radiation length of the target plate medium will be denoted by L. Recall that

$$T = \frac{\pi}{3}\frac{l}{\alpha L}\ , \tag{27}$$

where l is the thickness of the (collapsed) target. In analogy with the above, a total gap variable is introduced as

$$G = \frac{\pi}{3}\frac{g}{\alpha L}\ , \tag{28}$$

where g is the total width of all the gaps in the target.

Thus T measures the total radiation thickness of the material in the target while G measures the total thickness of the gaps. For example, a series of plots will be presented that compares the k spectrum for p and T fixed and G increasing. Of course in the BH limit of large k, and in the opposite limit of $l_f >> l$, F will not depend upon G. Sample numerical results will be presented in the next section for different gaps and number of plates.

8 Numerical Results

It is perhaps surprising that photons with energies in the tens of MeV can exhibit a macroscopic interference effect. In order to get a feel for this effect consider the

following. The radiation length for a gold target is L = 3.4mm. At a photon energy of 27MeV, and an incident electron beam of 25 GeV, the formation length

$$l_f = \frac{2xp}{m^2(1-x)} = \frac{2p_i p_f}{m^2 k} \tag{29}$$

is 0.034mm, the thickness of a 1% Au radiator. In lead, which has L = 5.6mm, the formation length corresponding to a 1% radiator occurs at a lower photon energy, 16MeV. The formation length also scales as the square of the incident electron energy.

In Figure 1 the photon spectra form factor for a 25 GeV electron beam incident upon a set of Au targets with T = 0.1, 1.0, and 10.0 (0.07, 0.7, and 7% of a radiation length respectively) are shown. The dashed curves are the form factor in the LPM approximation of Eq. (24). The solid curves will be discussed shortly. The computed points are shown and are simply connected by straight lines as in all the graphs.

In Figure 2 the form factor for a 25 GeV electron beam in the low k limit in which $l_f >> l$ is shown as a function of target thickness T. The behavior in the LPM approximation is also shown.

The first example of a structured target to be discussed is a T = 1 ($\sim$ 0.7% radiation thickness) target that is composed of two T = 0.5 laminations or plates. For this parameter set and for a gold target, the formation length is equal to the original target thickness at k = 42.4MeV. In Figure 3 the spectra are plotted for values of the gap extending out to G = 5. The subsidiary peak moves down in k as the gap increases. The peak occurs when the formation length matches the plate separation.

In Figure 4 the spectra expected from a 4-segment equally spaced Au target are given for several values of the gap. In this example, each plate has T = 0.25 for a total T = 1. The final total thickness of the target from the front surface to the rear surface at G = 9 is ten times the original thickness. The amount of radiator material

remains constant.

The interference effect persists for thicker targets. The spectra for a two plate Au target is plotted in Figure 5 for $T = 2$ and several gap values. For example, at $G = 5$ the total dimensionless distance between the centers of the plates is 6. The formation length is equal to this separation at $k \sim 42.4/6 \sim 7$ MeV which is roughly the position of the subsidiary peak.

The unexpected interference effect computed here should be straightforward to measure experimentally using the techniques pioneered in Ref. [5]. In addition, it may be possible to design structured targets to yield bremsstrahlung spectra with desirable and interesting characteristics.

9 Acknowledgements

I wish to thank Sid Drell, Peter Bested, Spencer Klein, and Ralph Becker-Szendy for discussions of the LPM effect and of the data taken by the SLAC E-146 collaboration.

References

[1] R. Blankenbecler and S. D. Drell, to be published in Phys. Rev. *D* in (1996). An extensive list of earlier references to the eikonal method are given here.

[2] H. A. Bethe and W. Heitler, Proc. Roy. Sot. *A146,* 83 (1934).

[3] L.D. Landau and I.J. Pomeranchuk, Dokl. Akad. Nauk. SSSR *92,* 535 (1953); *92,* 735 (1953). See also L. Landau, *The Collected Papers of L.D. Landau,* Sections 75-76, pp 586-593 Pergamon Press, (1965).

[4] A.B. Migdal, Phys. Rev. *103,* 1811 (1956).

[5] “An Accurate Measurement of the Landau, Pomeranchuk, Migdal Effect”, by P. Anthony et al., SLAC-PUB-95-6796. Phys. Rev. Lett. *75*, 1949 (1995).

[6] “Suppression of Radiation in an Amorphous Medium and in a Crystal”, N.F. Shul'ga and S.P. Komin, JETP Lett. *27*, 117 (1978).

[7] “Theory of Emission by Relativistic Particles in Amorphous and Crystalline Media”, N.V. Laskin, A.S. Mazmanishvili, N.N. Nasonov, and N.F. Shul'ga, JETP Lett. *62*, 438 (1985).

[8] “Radiation of Relativistic Particles in Single Crystals”, A.I. Akhiezer, N.F. Shul'ga, Sov. Phys. Usp. *25*, 541 (1982).

[9] “Semiclassical Theory of High-Energy Particle Radiation in External Fields,” A.I. Akiezer and N. F. Shul'ga, Physics Reports *234*, 297-365 (1993).

[10] R. Baier, Yu.L. Dokshitser, S. Peigne and D. Schiff, “ The Landau-Pomeranchuk-Migdal Effect in QED”, BI-TP 95-40, CERN-TH.96/14,CUTP-724, LPTHE-Orsay 95-84. Earlier references can be found here.

[11] “Notes on the Landau, Pomeranchuk, Migdal Effect: Experiment and Theory”, by Martin Perl, May 1994. SLAC-PUB-6514. Presented at “Les Rencontres de Physique de la Vallee d'Aoste”, La Thuile, Italy, 6-12 Mar 1994.

[12] R. Blankenbecler, “Multiple Scattering and Functional Integrals.” SLAC–PUB-96-7160, (to be published).

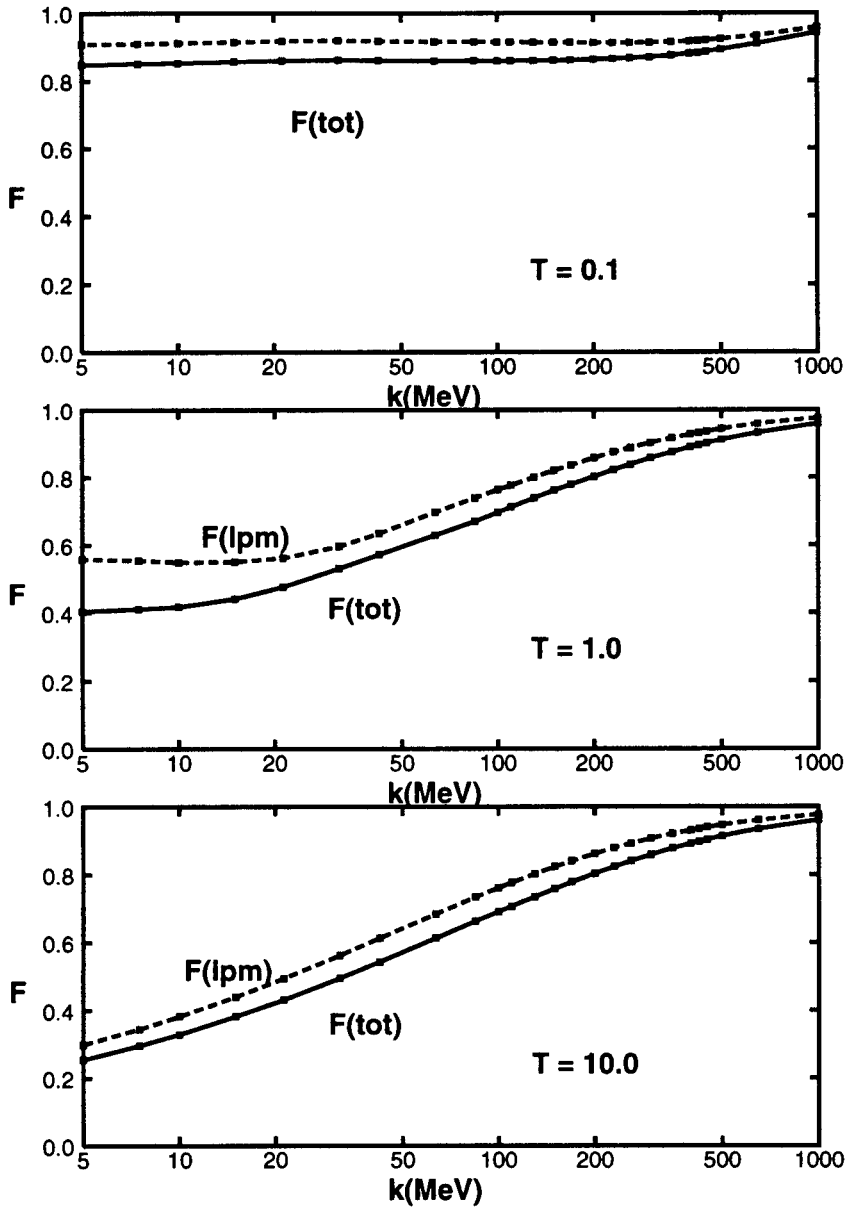

Figure 1

The form factor F(k,T=1,x) for a solid Au target for three different values of T. The dashed curves are the LPM approximation; the solid curves are the result with the cross correlation term.

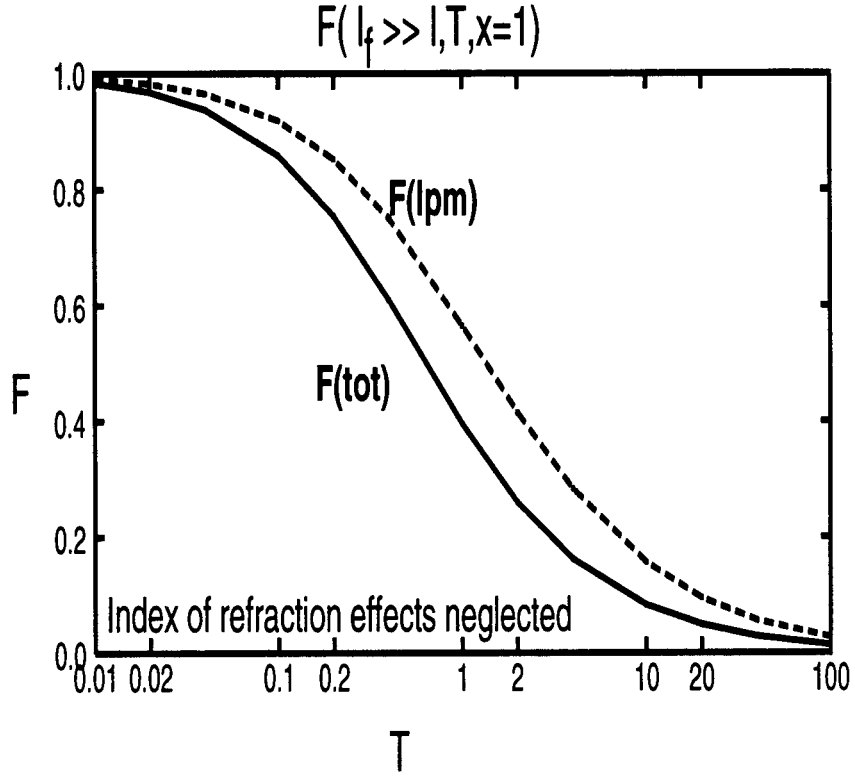

Figure 2

A plot of the formfactor F(k,T,x) vs T for small k, that is, for $l_f >> l$ and $x \sim 1$.

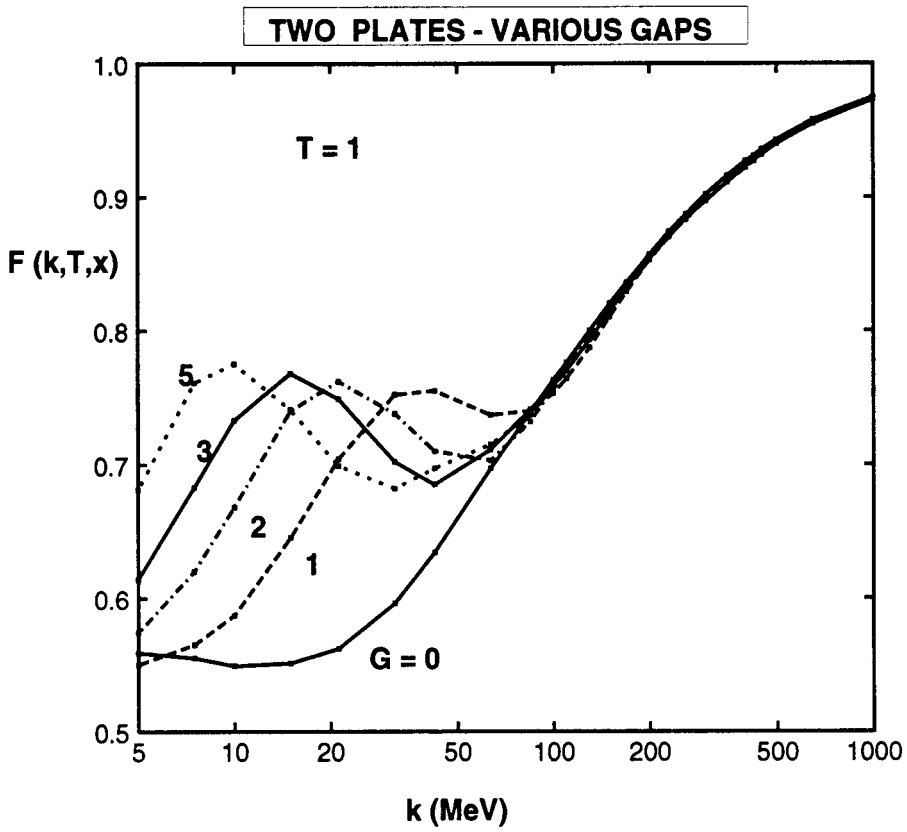

FIGURE 3

A summary graph of F(k,T=1,x) for a two segment Au target for various gap values in the LPM approximation.

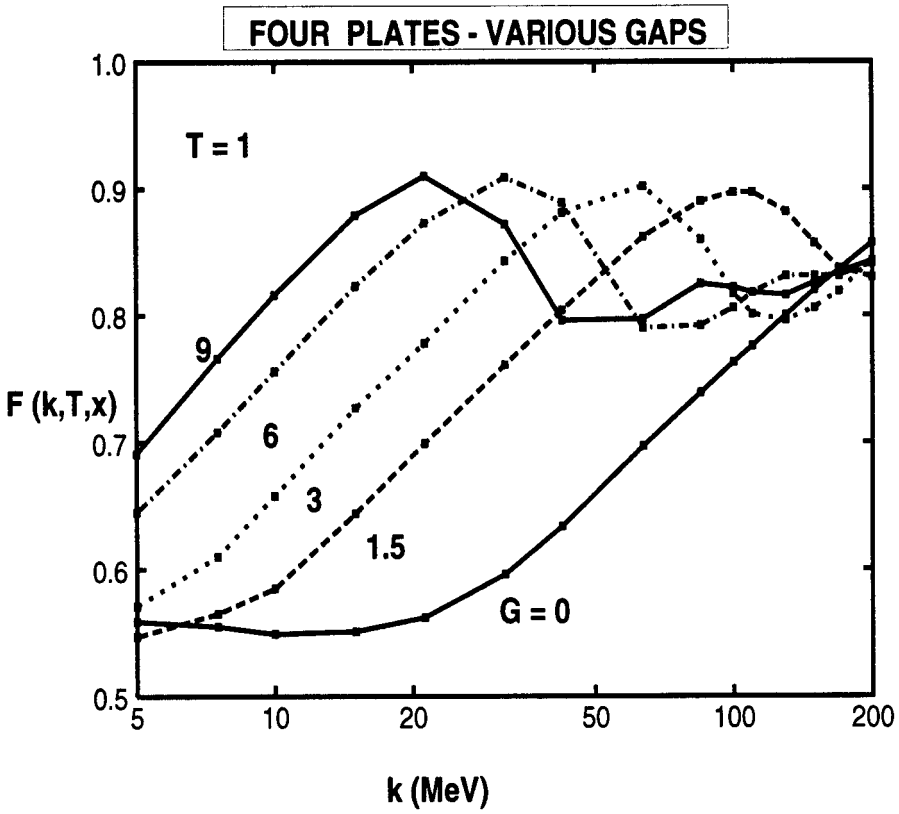

FIGURE 4

A summary graph of F(k,T=1,x) for a four segment Au target for selected gap values in the LPM approximation.

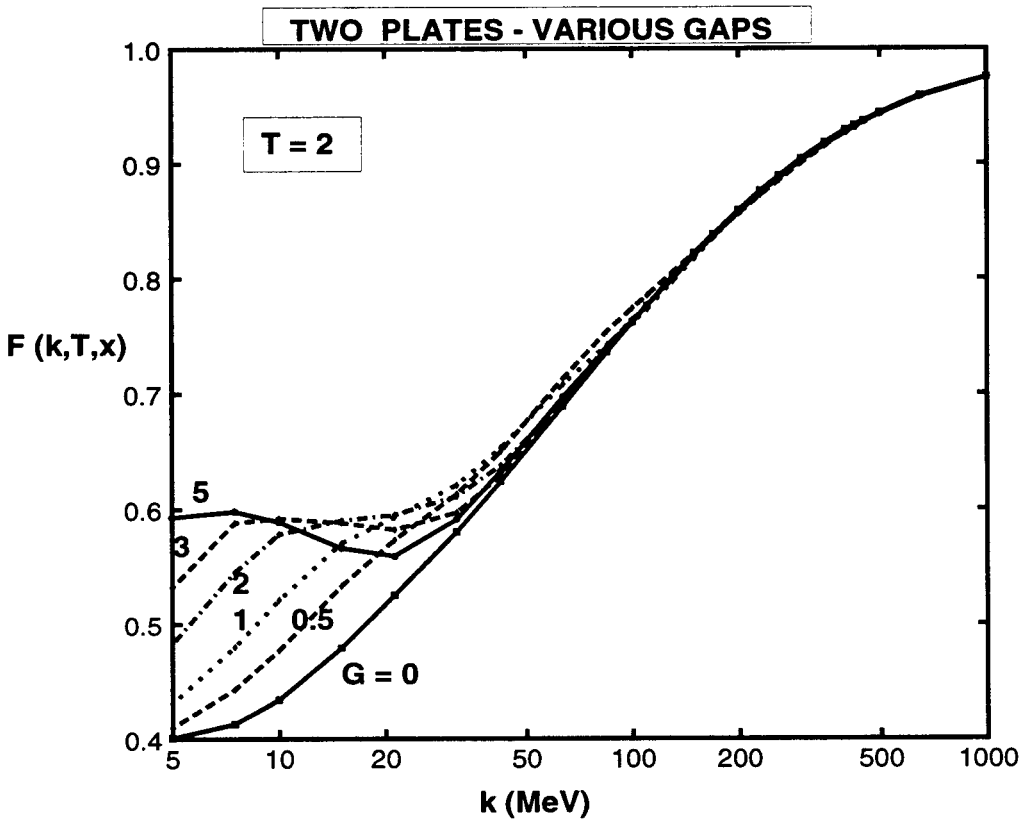

FIGURE 5

A summary graph of F(k,T=2,x) for a two segment Au target
for various gap values at an energy of 25 GeV
in the LPM approximation.